Optica Applicata, Vol. XLIX, No. 1, 2019
DOI: 10.5277/oa190102

Design of tunable multichannel filter in a one-dimensional photonic crystal incorporating uniaxial metamaterial at microwave frequency

BEHNAM KAZEMPOUR

Department of Physics, Ahar Branch, Islamic Azad University, Ahar, Iran; b-kazempour@iau-ahar.ac.ir

We proposed to design a tunable multichannel optical filter composed of uniaxial indefinite metamaterial and dielectric photonic crystal categories arrangement, which can be employed as a valuable variation of peak transmission in microwave frequency. Because of the optical axis and polarization dependence of the uniaxial metamaterial layer, the position trend in the multichannel optical filter is shown to also rely on both TE and TM polarizations. The numerical results show that by changes of the incidence angle, width of photonic band gap (PBG) compacts (widens) at TE (TM) polarization and the PBG of the structure shifts towards the higher frequency region, for both polarizations. In addition, the multichannel optical filter properties and shift trend of the PBG are also affected by changing the optical axis of the uniaxial indefinite metamaterial. Thus, results shown that without appending defect layer in this structure, the sets of comb-like resonant peaks in transmission modes can be utilized in the lower or higher band edge of PBG at TE and TM polarizations.

Keywords: uniaxial indefinite metamaterial, optical properties, multilayer design.

1. Introduction

During the last two decades, much consideration has been concentrated on the theoretical and experimental investigation of photonic crystals (PCs) or the photonic band gap (PBG) materials, due to encouraging demands of PCs in modern photonics devices [1, 2]. PCs are periodic layered materials and can contain frequency ranges in which the propagation of the electromagnetic waves is prohibited. These regions are labelled photonic band gaps (PBGs) [3, 4]. However, the PBGs depend upon some parameters, such as the optical and physical properties of the composed of PCs, filling fraction, kind of arrangements, angle of incidence and state of polarization. Hence, various compounds with different materials to produce a change of specialized functions for designing PCs are presented. Different elements, such as dielectrics, liquid crystals, ferroelectrics, metamaterials, and superconductors are applied in the form of photonic devices based on PC structures [5–10].

It is notable that a filter is much desired for multiplicity applications, specifically in photonic crystal circuits. When a defect layer is inserted into the periodic PCs structure, localized narrow bands are generated, which can be utilized for construction of filters with an exceptionally narrow transmission band. In most study, filters are focused on the PBGs manipulating, *i.e.*, all defect modes are designed to set within PBGs. Newly, a new class of filters based on PCs pass band have also excited researchers' considerable attention [7]. In comparison to conventional filters exerting the defect modes, current filters contain no defect layer, and can be demonstrated as $(AB)^N$. Here, one of the two elements can be employed as a superconductor, plasma, or single negative materials.

In the past, one-dimensional photonic crystals (1D PCs) containing double-negative (DNG) materials have attracted considerable of researches in the community. DNG materials with simultaneous negative permittivity ε and negative permeability μ in a special frequency region, have attracted extensive attention owing to their significant scientific abnormal peculiar properties [11–13]. DNG materials are now categorized as electromagnetic metamaterials and also PCs containing metamaterials are known as metamaterial photonic crystals [14]. Most studies of metamaterials are extensions based on the isotropic ones, while metamaterials initially manufactured in experiments are greatly anisotropic. Therefore, the permittivity and permeability should be studied as the tensors [15–18]. In comparison to isotropic PCs, the anisotropic metamaterials of PCs represent the exclusive optical properties such as: negative index of refraction, invisibility cloak, the utilized Brewster angle for both polarizations, and superlens that enable subwavelength far-field resolution are some potential applications of metamaterials [19–22]. Among the varieties of metamaterials, recently, indefinite materials are a kind of anisotropic metamaterials in which not all the principal elements of the permittivity and permeability tensors have the similar sign [23]. In fact, anisotropic left-handed materials are a specific reason of an indefinite medium [24, 25]. Also, experimental realization for manufacturing and characterization of the dispersive behavior in a uniaxial metamaterial exactly has been discussed in the past years [26, 27].

The optical properties and the Goos– Hänchen (GH) shift of a light wave structure of 1D PCs containing indefinite metamaterials have been examined recently [28–31]. The metamaterials have been introduced into PCs to obtain the filters that can be tuned by the structure period or the layer thickness [32–34]. These studies indicate that the manipulation of these filtering properties can be controlled by changing the number of period structures or the layer thickness [33, 35]. In contrast, only few works have been reported on the multichannel filter properties – using the anisotropic metamaterials and external parameters. However, the motivation to undertake this research resides in the fact that the authors have found no research on the influence of the orientation of the optical axis of the indefinite metamaterials and the incidence angle on the multichannel filtering properties without introducing any defect into the PCs.

In the present work, we would like to investigate the transmission properties of a 1D PC, which is composed of alternate layers of isotropic media and a uniaxial indefinite metamaterial. The calculations of the present study were carried out using the characteristics transfer matrix method for both TE and TM polarizations to the tunability of the multichannel filter. Our numerical results show that, due to the anisotropic metamaterial, the effect of the orientation of the optical axis of the anisotropic layers and the incidence angle on the modulation of the PBG and the trend shift frequency of the multichannel filter are studied. It will be shown that by increasing the incidence angle the blue-shift was observed in the PBGs, and the frequency positions of the multichannel filter can be manipulated by these parameters. In addition, the effects of the optical axis on the frequency position of the multichannel filter properties and the PBGs will be specifically explored for both polarizations. The results propose that a uniaxial indefinite metamaterial can be used to design the multichannel filter, and the shifting feature is dependent on the material.

2. Models and theory

We consider a 1D PC with the periodic structure embedded in air, as shown in Fig. 1. Here, B represents an isotropic dielectric layer with the permittivity ε_B, permeability μ_B, and thickness d_B, and A is a uniaxial indefinite metamaterial with thickness d_A; N is the period number, and a plane wave is incident at an angle θ upon the 1D PC from air. The interfaces of the layers are parallel to the x-y plane, and the z-axis is normal to the structure. We assume that the optical axis of the indefinite medium lies in the x-z plane and makes angle φ with the z-axis. In this case, the permittivity and permeability tensors of the indefinite metamaterial medium are shown in [29, 35, 36],

$$\varepsilon_A = \begin{pmatrix} P & 0 & F \\ 0 & \mu_\perp & 0 \\ F & 0 & W \end{pmatrix} \quad \text{and} \quad \mu_A = \begin{pmatrix} U & 0 & G \\ 0 & \mu_\perp & 0 \\ G & 0 & V \end{pmatrix} \tag{1}$$

where

$$P = \varepsilon_{A\perp}\cos^2\varphi + \varepsilon_{A||}\sin^2\varphi$$

$$W = \varepsilon_{A\perp}\sin^2\varphi + \varepsilon_{A||}\cos^2\varphi$$

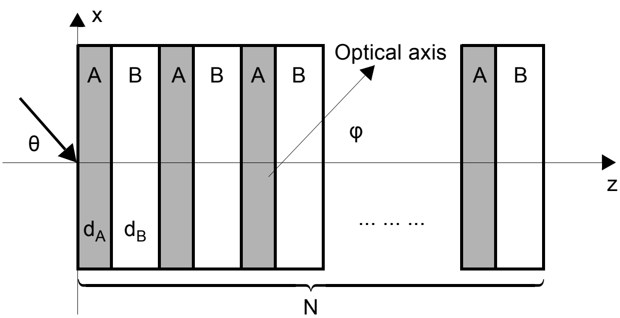

Fig. 1. Schematic of the proposed 1D PC consisting of alternate layers of isotropic material B and uniaxial indefinite metamaterial A; N is the number of periods.

$$F = -(\varepsilon_{A\perp} - \varepsilon_{A||})\cos\varphi\sin\varphi$$

$$U = \mu_{A\perp}\cos^2\varphi + \mu_{A||}\sin^2\varphi$$

$$V = \mu_{A\perp}\sin^2\varphi + \mu_{A||}\cos^2\varphi$$

$$G = -(\mu_{A\perp} - \mu_{A||})\cos\varphi\sin\varphi$$

Here, $\varepsilon_{A\perp}$, $\varepsilon_{A||}$, $\mu_{A\perp}$ and $\mu_{A||}$ are the principal elements of the permittivity and permeability tensors of the layer A along the optical axis and perpendicular to the optical axis, respectively, and φ is the angle between the optical axis and the z-direction. The permittivity and permeability of the layer A are complex given by [37]:

$$\varepsilon_{A\perp} = 1 - \frac{100}{\omega^2} \quad \text{and} \quad \mu_{A\perp} = 1 - \frac{200}{\omega^2} \tag{2}$$

where ω is the angular frequency of the incident light, and is measured in units of 10^9 rad/s. Consider an electromagnetic wave with frequency of ω, electric and magnetic fields of E and H, respectively, incident to the structure with angle θ with respect to the z-axis. The fundamental equations for an electromagnetic wave are given by the following Maxwell equations:

$$\nabla \times \mathbf{E}(\mathbf{r}, t) = i\omega\mu_0\boldsymbol{\mu}\mathbf{H}(\mathbf{r}, t) \quad \text{and} \quad \nabla \times \mathbf{H}(\mathbf{r}, t) = -i\omega\varepsilon_0\boldsymbol{\varepsilon}\mathbf{E}(\mathbf{r}, t) \tag{3}$$

where $\boldsymbol{\varepsilon}$ and $\boldsymbol{\mu}$ are the relative permittivity and permeability tensors, which, for anisotropic metamaterial with an arbitrary optical axis, are described in Eq. (1). At first, we focus only on the TE waves. According to the Maxwell equations, the electric field $\mathbf{E} = E_y(z)\exp[i(k_x x - \omega t)]\hat{\mathbf{j}}$ inside the indefinite layer satisfies the wave equation:

$$\frac{d^2E_y}{dz^2} + 2i\frac{G}{V}k_x\frac{dE_y}{dz} + \left(\frac{\omega^2}{c^2}\frac{\varepsilon_{A\perp}\mu_{A\perp}\mu_{A||}}{V} - \frac{U}{V}k_x^2\right)E_y = 0 \tag{4}$$

where $k_x = (\omega\sin\theta)/c$ is the vacuum wave vector. By imposing the continuity condition on E_y and H_x at the interfaces and introducing a wave function as,

$$\psi(z) = \begin{pmatrix} E_y \\ -\omega\mu_0 H_x \end{pmatrix} \tag{5}$$

The following relation is obtained between the electric and magnetic fields at any two positions z and $z + \Delta z$ of the same medium:

$$\psi(z) = M_A(\Delta z + \omega)\,\psi(z + \Delta z) \tag{6}$$

here, M_A is the transfer matrix of the indefinite medium,

$$M_{\mathrm{A}}(\Delta z+\omega) = \exp(i\alpha_1 z)\begin{pmatrix} \cos(\alpha_2\Delta z) & -\dfrac{i}{q_{\mathrm{A}}}\sin(\alpha_2\Delta z) \\ -iq_{\mathrm{A}}\sin(\alpha_2\Delta z) & \cos(\alpha_2\Delta z) \end{pmatrix} \tag{7}$$

and

$$\alpha_1 = \frac{G}{V}k_x$$

$$\alpha_2 = \frac{\omega}{c}\sqrt{\mu_{\mathrm{A}\perp}\mu_{\mathrm{A}||}\left(V\varepsilon_{\mathrm{A}\perp}-\frac{\sin^2\theta}{V^2}\right)}$$

$$q_{\mathrm{A}} = \frac{V\alpha_2}{\mu_{\mathrm{A}\perp}\mu_{\mathrm{A}||}\omega/c}$$

Similar results can be obtained for the isotropic layer B

$$M_{\mathrm{B}}(\Delta z+\omega) = \begin{pmatrix} \cos(k_z^{\mathrm{B}}\Delta z) & -\dfrac{i}{q_{\mathrm{B}}}\sin(k_z^{\mathrm{B}}\Delta z) \\ -iq_{\mathrm{B}}\sin(k_z^{\mathrm{B}}\Delta z) & \cos(k_z^{\mathrm{B}}\Delta z) \end{pmatrix} \tag{8}$$

where

$$k_z^{\mathrm{B}} = \frac{\omega}{c}\sqrt{\varepsilon_{\mathrm{B}}\mu_{\mathrm{B}}-\sin^2\theta}$$

is the z component of the wave vector in the medium B, c is the light speed in vacuum, and

$$q_{\mathrm{B}} = \frac{1}{\varepsilon_{\mathrm{B}}}\sqrt{\varepsilon_{\mathrm{B}}-\sin^2\theta}$$

For the TM waves, the wave equation in the metamaterial layer A can be obtained similarly as

$$\frac{\mathrm{d}^2H_y}{\mathrm{d}z^2}+2i\frac{F}{W}k_x\frac{\mathrm{d}H_y}{\mathrm{d}z}+\left(\frac{\omega^2}{c^2}\frac{\varepsilon_{\mathrm{A}\perp}\mu_{\mathrm{A}\perp}\mu_{\mathrm{A}||}}{W}-\frac{P}{V}k_x^2\right)H_y = 0 \tag{9}$$

here, M_{A} is the transfer matrix of the indefinite medium for TM polarization:

$$M_{\mathrm{A}}(\Delta z+\omega) = \exp(i\alpha_1 z)\begin{pmatrix} \cos(\alpha_2\Delta z) & -\dfrac{i}{q_{\mathrm{A}}}\sin(\alpha_2\Delta z) \\ -iq_{\mathrm{A}}\sin(\alpha_2\Delta z) & \cos(\alpha_2\Delta z) \end{pmatrix} \tag{10}$$

and

$$\alpha_1 = \frac{F}{W} k_x$$

$$\alpha_2 = \frac{\omega}{c} \sqrt{\varepsilon_{A\perp} \varepsilon_{A||} \left(W\mu_{A\perp} - \frac{\sin^2\theta}{W^2} \right)}$$

$$q_A = \frac{W\alpha_2}{\varepsilon_{A\perp} \varepsilon_{A||} \omega/c}$$

By means of the transfer matrix method [29], we obtain the transmission of the structure as,

$$T(\omega) = |t|^2 = \left| \frac{2p}{(M_{11} + M_{12}p)p + (M_{21} + M_{22}p)} \right|^2 \quad (11)$$

where, $p = \sqrt{k_0^2 - k_x^2}/k_0$, $M_{ij}(\omega)$ $(i, j = 1, 2)$ are the elements of the total matrix $M_N(\omega) = [M_A(d_A)M_B(d_B)]^N$.

3. Numerical results and discussions

In the following calculations, the material parameters to be used in the following calculations are: $\varepsilon_B = 3$, $\mu_B = 1$, $d_B = 10$ mm, $d_A = 5$ mm, $\varepsilon_{A||} = 1$, $\mu_{A||} = 1$ and $N = 30$ [36, 37]. The optical thickness of the layers was to be a quarter wave stack for ideal multilayer

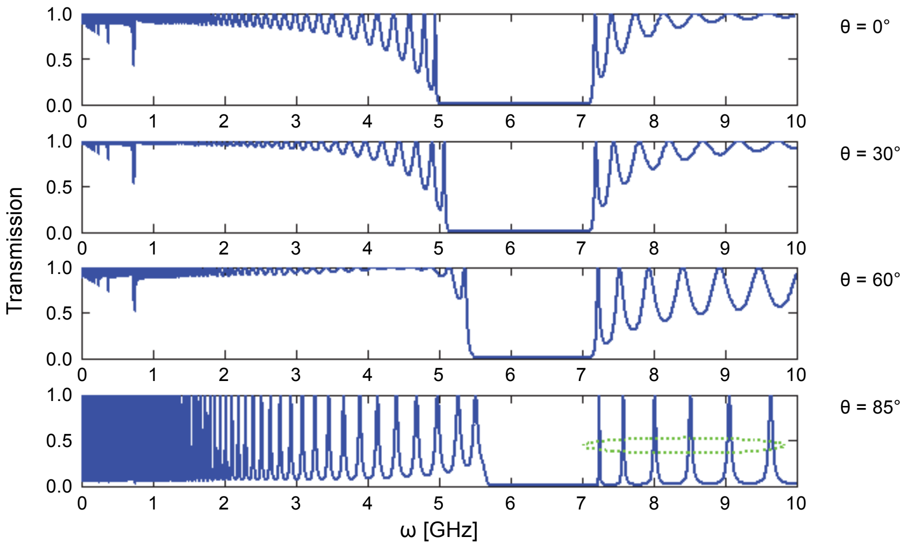

Fig. 2. Transmission spectrum of the 1D PC as a function of the angular frequency at four different incident angles when optical axis $\varphi = 0°$, under TE polarization.

arrangements: $n_A d_A = n_B d_B = \lambda_0/4$, where λ_0 is the so-called design wavelength usually as signed in the vicinity of center of PBG.

Now, we present the transmittance spectra for the proposed structure 1D PC. First, we investigate the effect of the incidence angle on the transmission spectra. In Fig. 2 we plot the transmittance spectra under the TE polarization at four different values of 0°, 30°, 60° and 85°. Here, we have taken the optical axis of indefinite metamaterial at φ = 0°. It is seen that, at θ = 0°, there exists a PBG whose band edges are at ω_L = 4.98 GHz and ω_H = 7.18 GHz, respectively. It is noted that the width of the PBG is decreased (compressed) compared to that of θ = 0° with the increase in the incidence angle from θ = 30° to θ = 60°. Additionally, as observable in the figure that the lower edge band gap shifts towards the high frequency side (blue shift), as the incident angle increases; whereas the higher edges band gap remains unchanged as the incident angle increases. Moreover, it is clear from figure that, by increasing the incidence angle, the sets of comb-like filter channels appear in the higher edge band gap.

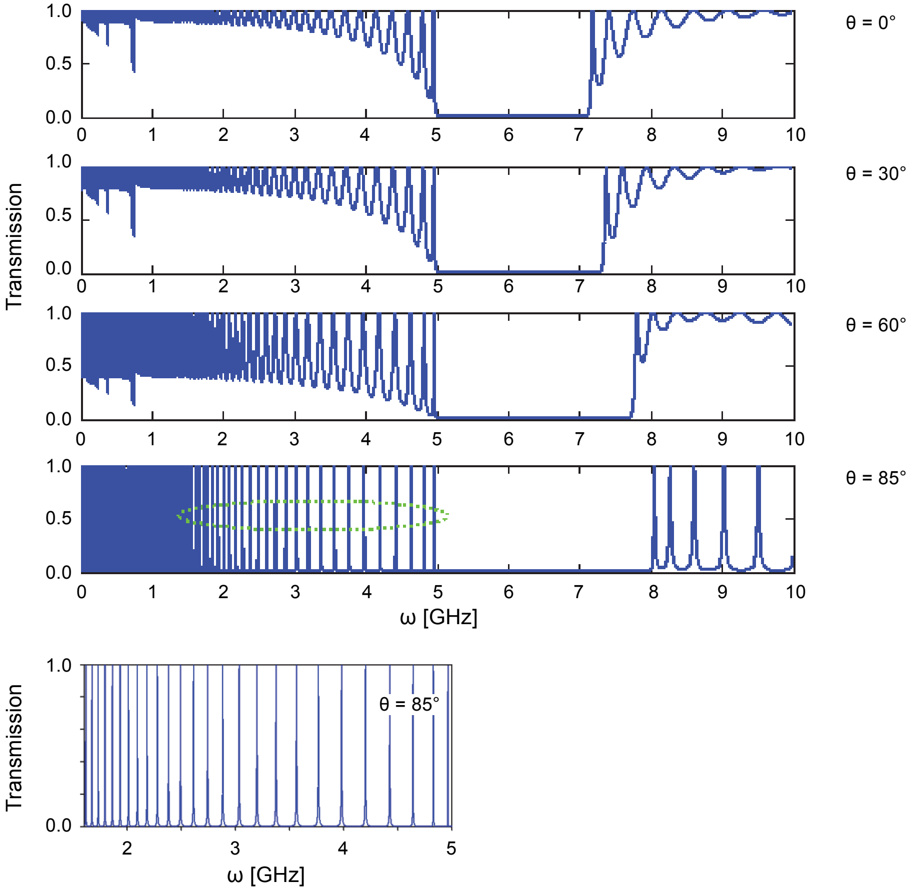

Fig. 3. Transmission spectrum of the 1D PC as a function of the angular frequency at four different incident angles when optical axis φ = 0°, under TM polarization.

Next, we would like to investigate how the tuning of the frequency position of the multichannel filters and tuning the PBGs are affected by adjusting the incidence angle under the TM polarization. In Fig. 3, we plot the transmission spectra at four different values of the incident angle $\theta = 0°$, 30°, 60° and 85°, for a specified value of the optical axis $\varphi = 0°$. The other parameters are same as those in Fig. 2. As illustrated, by increasing the incidence angle, the PBGs are shifted towards the higher frequency (blue shift), while the lower edge band gap has no sensible change, and the width of the PBG increases. Also, it is illustrated that, in the case of $\theta = 85°$, the sets of comb-like filter channels appear in the lower edge band gap. Therefore, the proposed structure can be used as an optical multichannel filter in this frequency range, which is enlarged in Fig. 3 in the frequency range (1.54 GHz < ω < 5.18 GHz). Another feature is of note that, under the TM polarization, the widths of the multichannel filters become narrow as the incidence angle increases, which indicates that the quality factor of the filter increases. This property will be useful for us to design the response frequencies of the multichannel filter.

To show the influence of φ on the transmission properties of the structure, a transmission spectrum is plotted for different values of the optical axis $\varphi = 0°$, 30°, 60° and 85°, for TE polarization, as illustrated in Fig. 4, at the normal incidence angle. The variation of the optical axis (Eq. (1)) results in non-zero off-diagonal elements of the dielectric permittivity and permeability tensor. The results show that by increasing the angle φ, a new gap as the angular gap band is observed in the lower frequency, and the PBGs appearing within the considered frequency region are blue-shifted. Also, it is evident from the figure that the position of the angular gap is unchanged as optical axis is larger than $\varphi = 30°$.

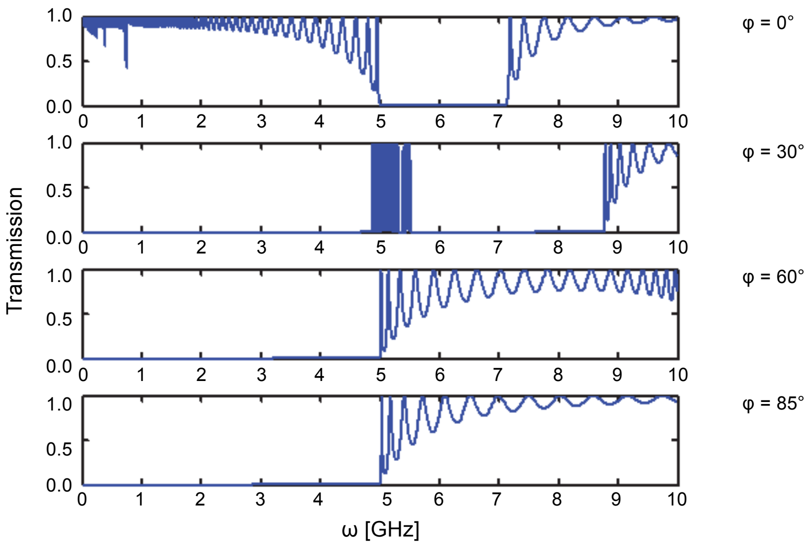

Fig. 4. Transmission spectrum of the 1D PC as a function of the angular frequency for different optical axis $\varphi = 0°$, 30°, 60° and 85°, for the normal incidence angle, under TE polarization.

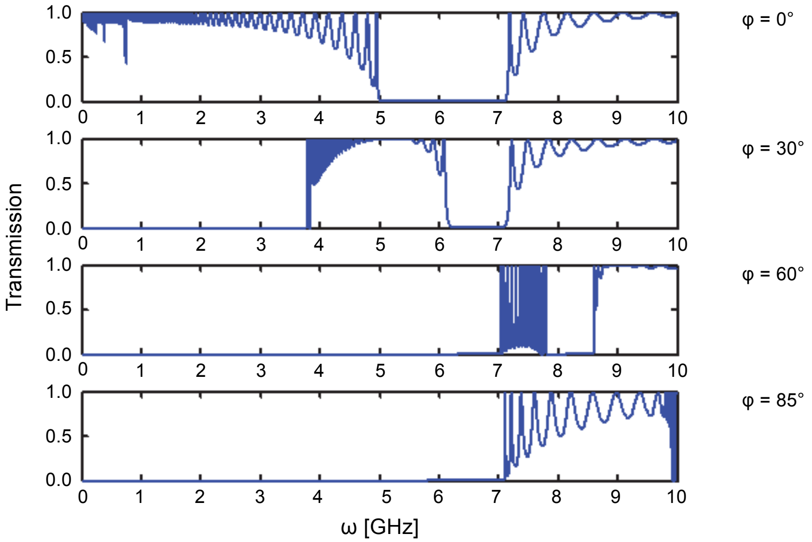

Fig. 5. Transmission spectrum of the 1D PC as a function of the angular frequency at four different optical axis $\varphi = 0°$, 30°, 60° and 85° for the normal incidence of the waves, under TM polarization.

Under the same conditions, we would like to investigate how the PBGs can be influenced by the optical axis under the TM polarized wave. The transmission spectrum for $\varphi = 0°$, 30°, 60° and 85° are depicted in Fig. 5. As observable, by increasing the optical axis, the PBG is blue-shifted. Moreover, the amount of shift in the PBG has a sensible change in the bandwidth of PBGs. Also, the bandwidth of PBGs decreases as the optical axis increases appreciably from $\varphi = 0°$ to 60°, and then nearly unchanged. For optical axis larger than $\varphi = 60°$, the PBG disappeared and in the lower frequency region, the angular gap band is seen. Therefore, it is evident from the figure that the transmission spectrum of the structure strongly depends on the value of φ. Specially in the higher values of φ, the transmission of the 1D PC was significantly reduced and finally the pass-bands in the lower given frequency side (from 0 to 7 GHz) are washed out.

Under the same conditions, we would like to investigate whether the transmission properties are affected by the optical axis for the normal angle of incidence. Figure 6 shows the effect of the optical axis four different values ($\varphi = 0°$, 30°, 60° and 85°) on transmission spectra, at the oblique incidence of light $\theta = 85°$, under the TE wave polarization. It can be seen that the transmission peaks are blue-shifted as φ increases, which means that such a filter possesses tunable working frequency. Meanwhile, the proposed structure at $\varphi = 30°$ can be utilized to design a multichannel filter in the higher frequency region, which is enlarged and attached in Fig. 6, at $\varphi = 60°$. Also, it is apparent that the position of the angular gap band is shifted toward the higher frequency from 0° to 30° and then nearly remains unchanged at angles larger than 60°. In addition, it can be observed from Fig. 6 that as the optical axis increases in the higher frequency region, the number of the transmission peaks increases and the width of the transmission mode becomes narrow, which illustrates that the quality factor of the filter raises.

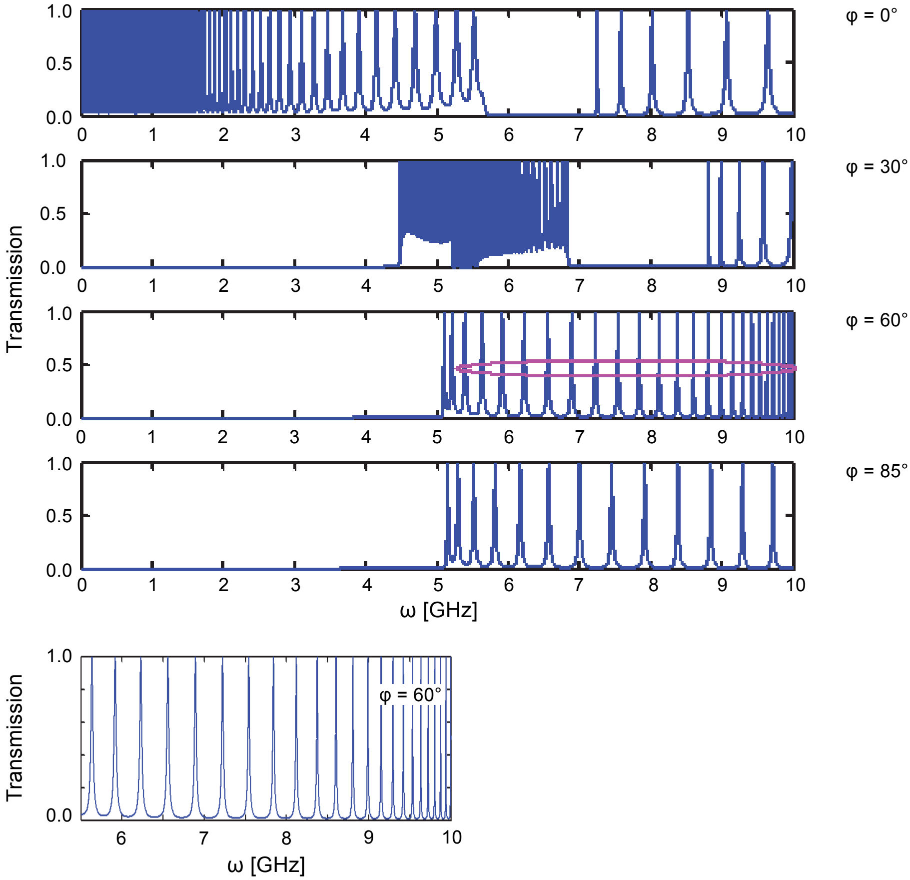

Fig. 6. Transmission spectrum of the 1D PC as a function of the angular frequency at four different optical axis $\varphi = 0°$, 30°, 60° and 85° at $\theta = 85°$, under TE polarization.

Finally, to show the effect of the optical axis φ on the tunability of the filtering properties such as the number, the widths and the positions of the transmission modes, under the TM polarization wave, are plotted in Fig. 7, for different optical axis $\varphi = 0°$, 30°, 60° and 85°. It is illustrated that, by increasing the optical axis, the PBGs appearing within the considered frequency region are blue-shifted. Also, it is found that as φ increases, the frequencies of the transmission peaks increase. Therefore, the proposed structure at $\varphi = 0°$ and $\varphi = 30°$ can be utilized to design a tunable multichannel filter in the lower frequency regions (in lower edge band gap), which are enlarged and attached in Fig. 7. Also, it can be seen from Fig. 7 that at $\varphi = 0°$ and $\varphi = 30°$ in the lower frequency region, the number of the transmission peaks increases as well as the width of the transmission modes becomes narrow and the separation of the filter decreases, which indicates that the quality factor of the filter increases. The amount of increasing quality factor for TM polarization is greater than for TE polarization, and the transmission peaks compress in the TM polarization. In addition, it is seen that the position

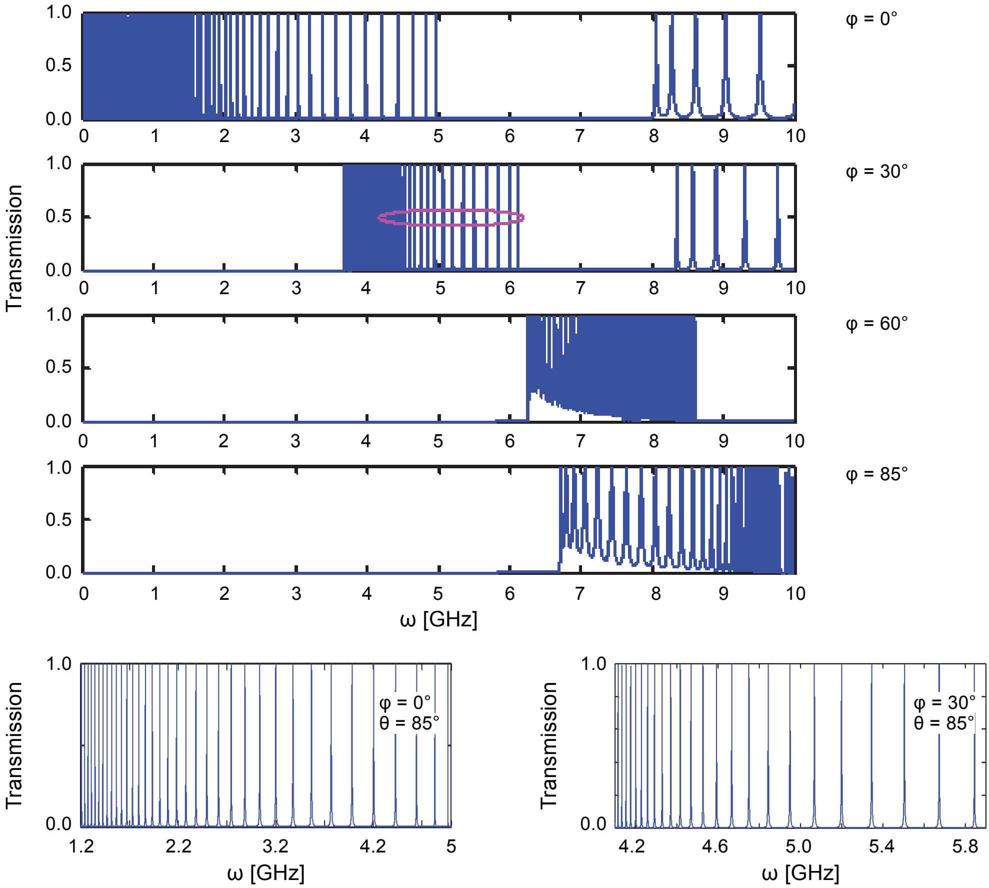

Fig. 7. Transmission spectrum of the 1D PC as a function of the angular frequency at four different optical axis $\varphi = 0°$, 30°, 60° and 85° at $\theta = 85°$, under TM polarization.

of the angular gap is shifted toward the higher frequency (blue shift) and the bandwidth of the angular gap increases as the optical axis φ increases. This transmission property indicates that the structure can be utilized for realizing a multichannel filter in different frequency ranges.

4. Conclusions

In this study, we have theoretically investigated the properties of the multichannel optical filter based on the uniaxial indefinite metamaterial-dielectric photonic crystal class arrangement. In comparison to the conventional optical filters, the results reveal that a multichannel filter can be achieved by using such a periodic structure without inserting any defect layer. The influence of variation in the optical axis and the incidence angle on the transmittance properties of the multichannel filter has been studied. Therefore, the orientation of the optical axis of the anisotropic medium and the incidence angle have a noticeable response only on the width, shift trend of the PBGs and filtering properties of the multichannel filter. Also, for oblique incidence, it is found that the position of the PBG is blue-shifted, as the incidence angle raises for both the TE and TM polarization. In addition to this, the bandwidth of the PBG can be narrowed for TE polarization while the width of the PBG is broadened for TM polarization, by increasing the incidence angle. Moreover, by adjusting the optical axis at a specified value of the incidence angle for TE polarization, the sets of comb-like filter channels appear in the higher edge band gap, whilst, for TM polarization, the sets of comb-like filter channels appear in the lower edge band gap.

References

[1] YABLONOVITCH E., *Inhibited spontaneous emission of photons in solid-state physics and electronics*, Physical Review Letters **58**(20), 1987, pp. 2059–2061, DOI: 10.1103/PhysRevLett.58.2059.

[2] JOHN S., *Strong localization of photons in certain disordered dielectric superlattices*, Physical Review Letters **58**(23), 1987, pp. 2486–2489, DOI: 10.1103/PhysRevLett.58.2486.

[3] HAITAO JIANG, HONG CHEN, HONGQIANG LI, YEWEN ZHANG, *Omnidirectional gap and defect mode of one-dimensional photonic crystals containing negative-index materials*, Applied Physics Letters **83**(26), 2003, pp. 5386–5391, DOI: 10.1063/1.1637452.

[4] CHIGRIN D.N., LAVRINENKO A.V., YAROTSKY D.A., GAPONENKO S.V., *Observation of total omnidirectional reflection from a one-dimensional dielectric lattice*, Applied Physics A **68**(1), 1999, pp. 25–28, DOI: 10.1007/s003390050849.

[5] GHRAATI A., ZARE Z., *Modeling of thermal tunable multichannel filter using defective metallic photonic crystals*, Optica Applicata **47**(4), 2017, pp. 611–619, DOI: 10.5277/oa170410.

[6] JAMSHIDI-GHALEH K., KAZEMPOUR B., PHIROUZNIA A., *Electrically tunable polarization splitting and conversion based on 1DPC structure with anisotropic defect layer*, Superlattices and Microstructures **101**, 2017, pp. 109–116, DOI: 10.1016/j.spmi.2016.11.041.

[7] PEINING LI, YOUWEN LIU, *Multichannel filtering properties of photonic crystals consisting of single -negative materials*, Physics Letters A **373**(21), 2009, pp. 1870–1873, DOI: 10.1016/j.physleta.2009.03.035.

[8] TAYA S.A., *P-polarized surface waves in a slab waveguide with left-handed material for sensing applications*, Journal of Magnetism and Magnetic Materials **377**, 2015, pp. 281–285, DOI: 10.1016/j.jmmm.2014.10.126.

[9] AGHAJAMALI A., BARATI M., *Effects of normal and oblique incidence on zero-$\bar{n}$ gap in periodic lossy multilayer containing double-negative materials*, Physica B: Condensed Matter **407**(8), 2012, pp. 1287–1291, DOI: 10.1016/j.physb.2012.01.125.

[10] JAMSHIDI-GHALEH K., KAZEMPOUR B., *Effect of incident angle and polarization on electrically-tunable defect mode in anisotropic photonic crystals*, Applied Optics **55**(16), 2016, pp. 4350–4356, DOI: 10.1364/AO.55.004350.

[11] TAYA S.A., *Dispersion properties of lossy, dispersive, and anisotropic left-handed material slab waveguide*, Optik **126**(14), 2015, pp. 1319–1323, DOI: 10.1016/j.ijleo.2015.04.013.

[12] TAYA S.A., SHAHEEN S.A., ALKANOO A.A., *Photonic crystal as a refractometric sensor operated in reflection mode*, Superlattices and Microstructures **101**, 2017, pp. 299–305, DOI: 10.1016/j.spmi.2016.11.057.

[13] TAYA S.A., *Theoretical investigation of slab waveguide sensor using anisotropic metamaterial*, Optica Applicata **45**(3), 2015, pp. 405–417, DOI: 10.5277/oa150312.

[14] SMITH D.R., PADILLA W.J., VIER D.C., NEMAT-NASSER S.C., SCHULTZ S., *Composite medium with simultaneously negative permeability and permittivity*, Physical Review Letters **84**(18), 2000, pp. 4184–4187, DOI: 10.1103/PhysRevLett.84.4184.

[15] Xiaoyong Hu, Zheng Liu, Qihuang Gong, *Tunable multichannel filter in photonic crystal heterostructure containing permeability-negative materials*, Physics Letters A **372**(3), 2008, pp. 333–339, DOI: 10.1016/j.physleta.2007.07.029.
[16] Wang Z.P., Wang C., Zhang Z.H., *Goos–Hänchen shift of the uniaxially anisotropic left-handed material film with an arbitrary angle between the optical axis and the interface*, Optics Communications **281**(11), 2008, pp. 3019–3024, DOI: 10.1016/j.optcom.2008.01.055.
[17] Kazempour B., Jamshidi-Ghaleh K., Shabzendeh M., *Transmittance properties of tunable filter in a 1D photonic crystal doped by an anisotropic metamaterial*, Superlattices and Microstructures **109**, 2017, pp. 708–715, DOI: 10.1016/j.spmi.2017.05.062.
[18] Yeh P., *Optical Waves in Layered Media*, Wiley, 1988.
[19] Jacob Z., Alekseyev L., Narimanov E., *Optical hyperlens: far-field imaging beyond the diffraction limit*, Optics Express **14**(18), 2006, pp. 8247–8256, DOI: 10.1364/OE.14.008247.
[20] Yuanjiang Xiang, Xiaoyu Dai, Shuangchun Wen, Dianyuan Fan, *Properties of omnidirectional gap and defect mode of one-dimensional photonic crystal containing indefinite metamaterial with hyperbolic dispersion*, Journal of Applied Physics **102**(9), 2007, article ID 093107, DOI: 10.1063/1.2809446.
[21] Guanghao Zhu, *Designing a square invisibility cloak using metamaterials made of stacked positive -negative index slabs*, Journal of Applied Physics **113**(16), 2013, article ID 163103, DOI: 10.1063/1.4802446.
[22] Zi Jing Wong, Yuan Wang, O'Brien K., Junsuk Rho, Xiaobo Yin, Shuang Zhang, Fang N., Ta-Jen Yen, Xiang Zhang, *Optical and acoustic metamaterials: superlens, negative refractive index and invisibility cloak*, Journal of Optics **19**(8), 2017, article ID 084007, DOI: 10.1088/2040-8986/aa7a1f.
[23] Freeman D., Madden S., Luther-Davies B., *Fabrication of planar photonic crystals in a chalcogenide glass using a focused ion beam*, Optics Express **13**(8), 2005, pp. 3079–3086, DOI: 10.1364/OPEX.13.003079.
[24] Yuanjiang Xiang, Xiaoyu Dai, Shuangchun Wen, *Omnidirectional gaps of one-dimensional photonic crystals containing indefinite metamaterials*, Journal of the Optical Society of America B **24**(9), 2007, pp. 2033–2039, DOI: 10.1364/JOSAB.24.002033.
[25] Tao Pan, Guo-Ding Xu, Tao-Cheng Zang, Lei Gao, *Study of a slab waveguide loaded with dispersive anisotropic metamaterials*, Applied Physics A **95**(2), 2009, pp. 367–372, DOI: 10.1007/s00339-008-5061-6.
[26] Dexin Ye, Shan Qiao, Jiangtao Huangfu, Lixin Ran, *Experimental characterization of the dispersive behavior in a uniaxial metamaterial around plasma frequency*, Optics Express **18**(22), 2010, pp. 22631–22636, DOI: 10.1364/OE.18.022631.
[27] Wen-Jie Chen, Shao-Ji Jiang, Xiao-Dong Chen, Baocheng Zhu, Lei Zhou, Jian-Wen Dong, Chan C.T., *Experimental realization of photonic topological insulator in a uniaxial metacrystal waveguide*, Nature Communications **5**, 2014, article ID 5782, DOI: 10.1038/ncomms6782.
[28] Pursiainena O.L.J., Baumberg J.J., *Compact strain-sensitive flexible photonic crystals for sensors*, Applied Physics Letters **87**(10), 2005, pp. 101902–101904, DOI: 10.1063/1.2032590.
[29] Tao Pan, Guoding Xu, Taocheng Zang, Lei Gao, *Goos–Hänchen shift in one-dimensional photonic crystals containing uniaxial indefinite medium*, Physica Status Solidi B **246**(5), 2009, pp. 1088–1093, DOI: 10.1002/pssb.200844430.
[30] Shu W., Ren Z., Luo H., Li F., *Brewster angle for anisotropic materials from the extinction theorem*, Applied Physics A **87**(2), 2007, pp. 297–303, DOI: 10.1007/s00339-006-3832-5.
[31] Saleki Z., Entezar S. R., Madani A., *Optical properties of a one-dimensional photonic crystal containing a graphene-based hyperbolic metamaterial defect layer*, Applied Optics **56**(2), 2017, pp. 317 –323, DOI: 10.1364/AO.56.000317.
[32] Chun-zao Li, Shao-bin Liu, Xiang-kun Kong, Bo-rui Bian, Xue-yong Zhang, *Tunable photonic bandgap in a one-dimensional superconducting-dielectric superlattice*, Applied Optics **50**(16), 2011, pp. 2370–2375, DOI: 10.1364/AO.50.002370.

[33] KUN-YUAN XU, XIGUANG ZHENG, CAI-LIAN LI, WEI-LONG SHE, *Design of omnidirectional and multiple channelled filters using one-dimensional photonic crystals containing a defect layer with a negative refractive index*, Physical Review E **71**(6), 2005, article ID 066604, DOI: 10.1103/PhysRevE.71.066604.

[34] WU C.-J. , LEE M.-H., JIAN J.-Z., *Design and analysis of multichannel transmission filter based on the single-negative photonic crystal*, Progress in Electromagnetics Research **136**, 2013, pp. 561–578, DOI: 10.2528/PIER12122202.

[35] SCHURIG D., SMITH D.R., *Spatial filtering using media with indefinite permittivity and permeability tensors*, Applied Physics Letters **82**(14), 2003, pp. 2215–2217, DOI: 10.1063/1.1562344.

[36] SMITH D.R. KROLL N., *Negative refractive index in left-handed materials*, Physical Review Letters **85**(14), 2000, pp. 2933–2936, DOI: 10.1103/PhysRevLett.85.2933.

[37] JENSEN LI, LEI ZHOU, CHAN C.T., SHENG P., *Photonic band gap from a Stack of positive and negative index materials*, Physical Review Letters **90**(8), 2003, article ID 083901, DOI: 10.1103/PhysRevLett.90.083901.

Received January 8, 2018
in revised form April 10, 2018